Lab on a Chip

Miniaturisation for chemistry, physics, biology, materials science and bioengineering

www.rsc.org/loc

Volume 12 | Number 14 | 21 July 2012 | Pages 2423–2586

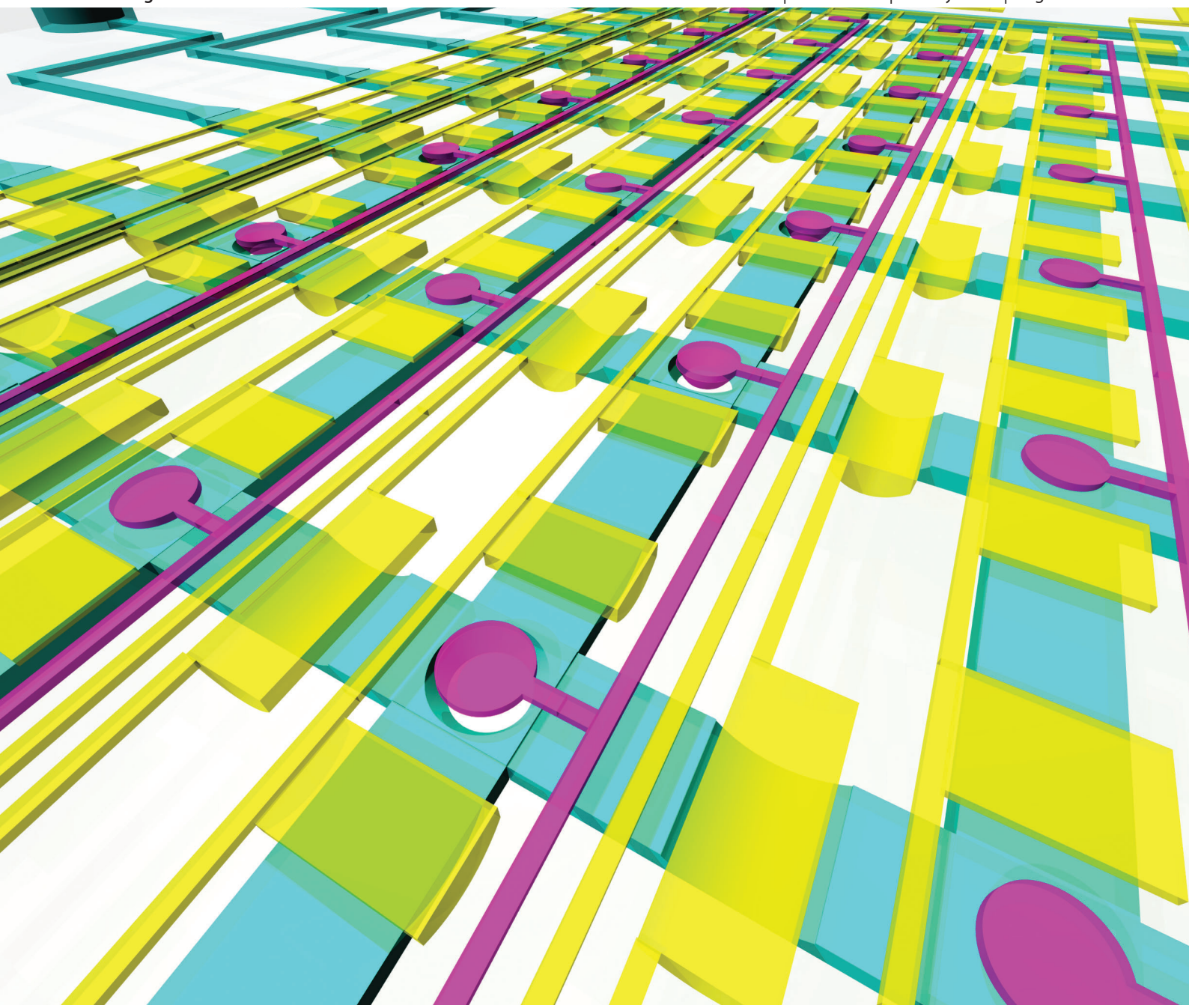

ISSN 1473-0197

RSC Publishing

COMMUNICATION

Yanyi Huang *et al.*

High-throughput immunoassay through in-channel microfluidic patterning

Lab on a Chip

Dynamic Article Links

Cite this: *Lab Chip*, 2012, **12**, 2487–2490

www.rsc.org/loc

COMMUNICATION

High-throughput immunoassay through in-channel microfluidic patterning†

Chunhong Zheng,[ab] Jingwen Wang,[a] Yuhong Pang,[ab] Jianbin Wang,[a] Wenbin Li,[c] Zigang Ge*[a] and Yanyi Huang*[ab]

Received 9th February 2012, Accepted 26th March 2012
DOI: 10.1039/c2lc40145b

We have developed an integrated microfluidic immunoassay chip for high-throughput sandwich immunoassay tests. The chip creates an array of reactive patterns through mechanical protection by actuating monolithically embedded button valves. We have demonstrated that this chip can achieve highly sensitive immunoassay tests within an hour, and requires only microliter samples.

Immunoassays, including enzyme-linked immunosorbent assays (ELISAs) and other related assays, are important techniques for biochemical analysis and diagnostic detection.[1,2] Traditional immunoassay experiments, carried out on multi-well plates, take several hours to complete because of the hour-long incubation time for most steps. Consumption issues also remain a challenge for tests with precious samples and antibody reagents. In addition, immunoassays usually require sophisticated instruments and skilful operations to obtain reliable results. Recently, the rapid development of microfluidic technologies, also known as "lab-on-a-chip" technologies, has enabled the miniaturization of various chemical or biochemical reactions onto tiny devices.[3,4] For immunoassays, microfluidic devices present great advantages, including decrease of consumption, reduction of experimental time, increasing of throughput, and convenient operation.[5,6] Methods utilizing capillary electrophoresis,[7] spinning CD-like disks,[8] and magnetic beads[9] have been reported to perform high-throughput immunodetection.

Poly(dimethylsiloxane) (PDMS) has become the most popular material with which to fabricate microfluidic devices for bioanalysis as this low-cost elastomer is easily molded into complex liquid channels and monolithically embedded valves for flow control.[10] Several PDMS devices have been applied to immunoassays. Detection using fluorescence images,[11] label-free surface plasmon resonance[12] or confocal imaging[13] provides excellent sensitivity but requires complicated or expensive instrumentation. Highly sensitive detection of HIV and other antigens from multiple samples can be achieved in parallel through PDMS slabs with microchannels and proper substrate material for protein adsorption.[14,15]

Surface patterning is a practical and popular method that can easily be applied to many high-throughput and small-volume biological applications to create functional surfaces for controllable chemical reactions,[16,17] microarrays or spots of biomolecules,[18,19] and well orientated single molecules.[20] Many patterning approaches, including widely-used micro-contact printing,[21–23] have been reported to create colonies for cell culture and coculture,[24,25] cell transfection,[26,27] drug screening,[24] stem cell differentiation,[28] and many other studies based on single cells.[29] However, for most of these methods that pattern openly-accessible surfaces with limited integration and automation, careful operations are essential to eliminate contaminations.

Here we report a novel method to pattern the microfluidic channels through mechanical blocking *in situ*. With the simple and robustly-created patterns, our integrative microfluidic chip performs high-throughput fluorescence sandwich immunoassays using less than 1 μl antibody solution and with a detection limit lower than 10 pg ml^{-1} for clinical samples.

The device, shown in Fig. 1, contains 32 reaction chambers for immunoassay detection in parallel. The volume of each chamber is 2 nl. The chip is made from PDMS through multi-layer soft lithography[30] on an epoxide glass slide. Each chamber has a round shape button valve, the critical component for chip function originated from the "MITOMI" chips.[31] The chambers are formed by segmenting microfluidic channels with a series of embedded pneumatic valves. These isolation valves can be divided into two major groups, longitudinal valves and horizontal ones. Each chamber is formed by two pairs of valves that isolate the button. When pressure is applied to the button, the deformable PDMS membrane will partially cover the channel since the button diameter is smaller than channel width. The activation of buttons does not block the liquid flow in the microfluidic channels completely. Therefore, only certain area in the channel is mechanically blocked, preventing liquid access. We have designed multiple inlets with gating valves to introduce common reagents, including washing buffer, blocking buffer, capture antibodies, and detecting antibodies. Samples are brought into the chip through another set of inlets. Each reaction chamber needs only a few

[a]*College of Engineering, Peking University, Beijing, 100871, China. E-mail: yanyi@pku.edu.cn (Y.H.); gez@pku.edu.cn (Z.G.)*
[b]*Biodynamic Optical Imaging Center (BIOPIC), Peking University, Beijing, 100871, China*
[c]*Beijing Shijitan Hospital, Capital Medical University, Beijing, 100038, China*

† Electronic Supplementary Information (ESI) available: Experimental details and supporting figures. See DOI: 10.1039/c2lc40145b/

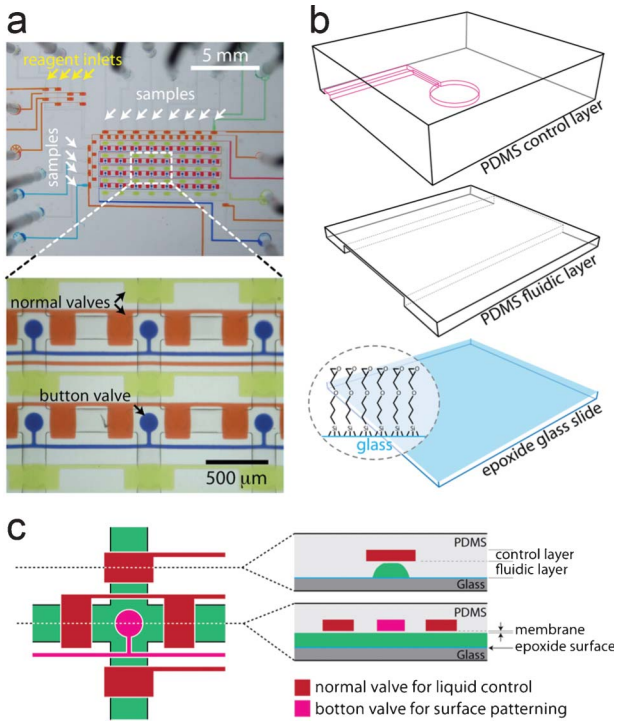

Fig. 1 The microfluidic immunoassay chip and the construction of the button valves. (a) The microphotographs of a chip with inlets for introducing reagents and samples. Normal valves are used to create the small reaction chambers, while the button valves are used to pattern the epoxide surface. The chip is filled with dyes to illustrate different layers. (b) The layered structure of the device. (c) The top-view and side-views of a reaction chamber unit.

nanoliter solutions for each step of the experiment, with a total consumption of antibody solution less then 1 μl for most reactions.

The workflow of immunoassay on-chip is shown in Fig. 2. For sandwich immunoassay, we first activated the buttons to protect the reaction spots, and then incubated the whole channel with bovine serum albumin (BSA) based blocking buffer. In the blocking buffer accessible region, the proteins reacted covalently

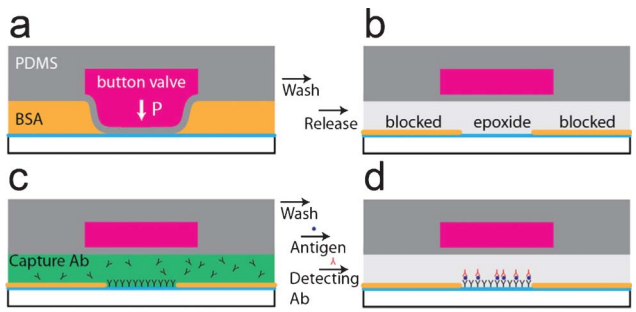

Fig. 2 Workflow of the device and pattern formation. (a) Under pressure, the bottom PDMS membrane of the button deforms and partially blocks the channel. When the BSA blocking buffer is introduced into the channel, the uncovered surface will be blocked. (b) After releasing the button, the previously protected pattern becomes reactive sites. (c) During the sandwich fluorescence ELISA, the mechanically patterned reaction area is modified with capture antibody for antigen binding. (d) The detecting antibody selectively binds to antigen, leading to detectable fluorescence signal.

with epoxide to prevent further chemical modification on the slide. The excess blocking buffer was then flushed away by phosphate-buffered saline (PBS), the washing buffer. After releasing the buttons, the protected regions with intact epoxide groups were exposed. We bonded the capture antibody to the mechanically patterned spots by incubating with antibody solution (500 μg ml^{-1}) for 15 min. After another PBS washing, we added the sample for binding. We employed the Fluorescein isothiocyanate (FITC)-conjugated detecting antibody and detected the fluorescence signal coming out of the patterned spots. We carried out our detection using a fluorescence microscope equipped with a CCD camera. Excited with blue light at 490 nm, the green emission (520 nm) of the chip was imaged and then analyzed with Image J.[32] The intensity of the serum-blocked areas, generated from non-specific binding, was used for background subtraction. Compared with previous approaches using controllable microfluidic devices, the major advantage of our design is that the patterned spots provide identical reaction conditions for all tests on-chip, with fixed location of each spot for signal detection and the adjacent area for background correction.

The buttons are circular in design so that pressure is distributed symmetrically. The size of the reaction area patterned by the buttons is mainly decided by the pressure applied (Fig. S1†). Over-pressurized (>0.25 MPa) buttons will interfere with liquid flow, while under-pressurized (<0.05 MPa) buttons block insufficient portions of the channels and the patterning is less stable, leading to low sensitivity and reproducibility.

Protein-surface binding is a key factor for sandwich immunoassays. Although physical adsorption of protein molecules on PDMS surface have been applied to immunodetection,[13] we find that epoxide-reactive glass substrates are still the optimal choice. We use FITC-conjugated human IgG to compare the binding performances of PDMS and that of epoxide glass substrates (Fig. S2a†). PDMS offers similar detection limits as the epoxide slide does, but the irreversible covalent attachment of proteins on the epoxide surface provides better robustness and controllability than the reversible van der Waals interactions between proteins and the PDMS surface.[33,34]

During the patterning process, blocking buffer covers whole surface except the patterns protected by actuated buttons. Formulation of the blocking buffer affects the fluorescent background. We have tested four formulas: PBS, PBS with 1% BSA, PBS with 1% BSA and 10 mM Tris buffered saline, and PBS with 1% BSA and 20% polyethylene glycol (PEG-2000). We incubated the micro-channels with blocking buffer for 10 min, and then with FITC-labeled goat anti-human IgG for 15 min. Fluorescence images show that BSA indeed blocks the surface and Tris is essential to facilitate the blocking performance and to lower the background (Fig. S2b†). We found that the reaction buffer is also critical to the performance of sandwich immunoassays. Carbonate buffer solution (CBS, pH 9.6) ensures stable coupling between proteins and epoxide glass slides (Fig. S2c†) and generate more stable conditions for immunoassays. We found that 15 min is sufficient for stable binding between proteins and substrates. Over-adsorption may introduce artifacts into the concentration determination (Fig. S2d†). The concentration of capture antibody is highly related to the detection limit in our sandwich immunoassay (Table S1†). The higher the concentration of capture antibody, the lower the detection limit. Therefore, we

can design the proper protocol to match the sensitivity and dynamic range required for detecting specific antigens. We chose 500 μg ml^{-1} capture antibody and reached the detection limit as low as 0.02 ng ml^{-1}.

Proper concentration of detecting antibody is determined by checkerboard titration (Fig. S3†). The concentration should be high enough to boost the sensitivity of the immunoassay. However, high concentration will directly lead to high background intensity, resulting in unreliable measurement of antigen at low concentration. We found that 125 μg ml^{-1} detecting antibody solution provided proper balance between sensitivity and background intensity.

Through these trials the final experimental protocol has been optimized. The whole experiment is performed at 25 °C. We first blocked non-reactive areas with blocking buffer (PBS with 1% BSA and 10 mM Tris buffered saline) for 10 min with the button activated. After PBS washing, the buttons were inactivated and the unprotected button area is treated with 500 μg ml^{-1} capture antibody for 15 min. After another PBS washing, we introduced the sample and incubated for 15 min. We then washed the channels with PBS, and incubated the channels with 125 μg ml^{-1} detecting antibody for 10 min. The images were taken after the final PBS washing.

The performance of the chip is firstly evaluated by FITC-conjugated human IgG through a direct binding assay. After the blocking step, all buttons were released and the proteins with different concentrations were injected into channels to react with the pattern with epoxide groups exposed. The linear relationship between the spot intensity and the FITC–IgG concentration is shown in Fig. 3, with a dynamic range over 10^4. Since direct binding assay was usually not reliable enough for immunodetection, we then tested the performance of sandwich immunoassay using this device by coupling the mouse anti-human IgG monoclonal antibody onto the epoxide spots, capturing human IgG (antigen) with different concentrations, and then using FITC-conjugated rabbit anti-human IgG polyclonal antibody as the detecting antibody to measure the fluorescence intensity of each spot (Fig. S4†). The chip could perform with a detection limit as low as 1 pg ml^{-1}, with a linear dynamic range from 1 pg ml^{-1} to 10 ng ml^{-1} (Fig. 3c). This range is ideal for many biomarkers detection at physiologically relevant concentrations.

We designed an improved version of the device, with more reaction chambers (Fig. S5†), for sandwich immunoassay detection of carcinoembryonic antigen (CEA) from human serum samples. Elevated CEA levels in human serum (>2.5 ng ml^{-1}) can serve as a diagnostic marker for colon, lung and breast cancers.[35] Fast and sensitive measurement of CEA level can facilitate the early detection of cancers. We chose mouse anti-human CEA monoclonal antibody as capture antibody, and rabbit anti-human CEA polyclonal antibody as detection antibody. Results (Fig. 4) show the linear dynamic range from 10 pg ml^{-1} to 1 μg ml^{-1}. Six serum samples from patients were used for analyzing CEA level with our immunoassay chip. Fig. 4b shows the images of button spots and different samples had different fluorescence intensities. The result of our approach agrees very well with the control experiments performed with conventional sandwich immunoassay using microwell-plates. The error bars of our chip-based measurement are smaller than those of conventional method, indicating the excellent robustness and reproducibility of this chip-based device

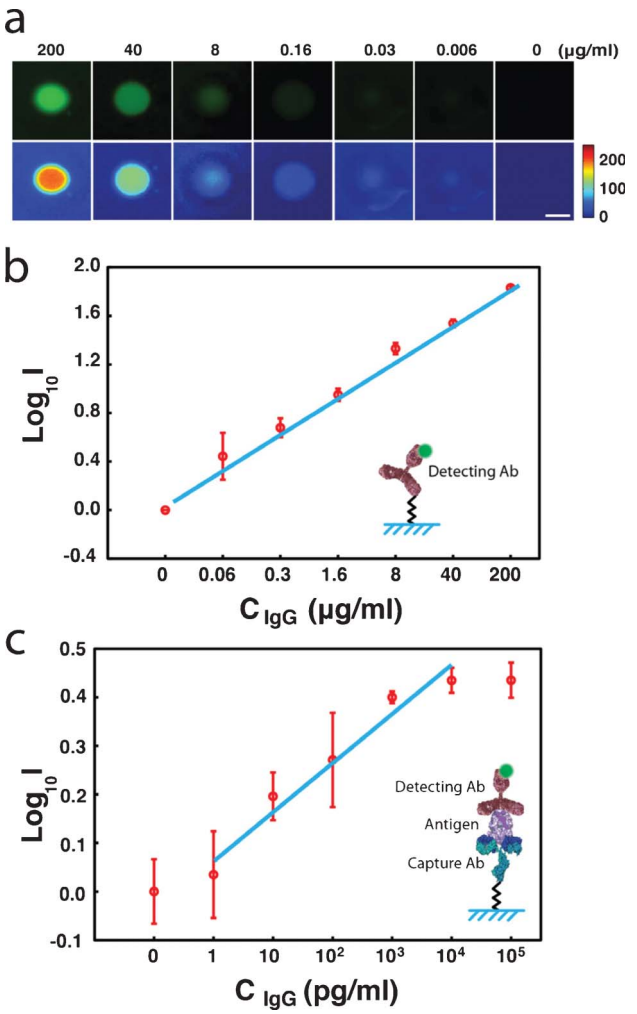

Fig. 3 The immunoassay result using model systems. (a) The fluorescence images of FITC–human IgG coupled onto the mechanically patterned substrate. The upper row is the original images and the lower row is the corresponding color map of the intensity. Scale bar is 100 μm. (b) The fluorescence intensity is linearly related to IgG concentration (n = 3). (c) The fluorescence sandwich immunoassay detection of human IgG antigen (n = 3) at different concentrations. The data presented in (b) and (c) are background subtracted.

(CV = 10%). Moreover, in contrast with the conventional 20 μl sample consumption for a single test and 6 h experimental time, our method requires less than 1 μl serum for four experimental replicates in parallel, and finishes the assay within 1 h. This reduction of experimental time, due to the highly confined volume of reaction, greatly facilitates the sandwich immunoassay application in clinical diagnostics and point-of-care testing, and it has the potential to become a routine, rapid biochemical analysis technique.

In conclusion, we have developed a novel microfluidic device to perform high-throughput ELISA measurements with mere 1 μl of each sample for four repeats, and a 1 h total experimental time. The reaction pattern created by mechanical protection efficiently binds the capture antibodies, offering reliable and robust substrate to perform sandwich fluorescence ELISA. We have achieved a linear dynamic range over 5 logs and the detection limit at 10 pg ml^{-1} for CEA measurement. Applying our method to serum

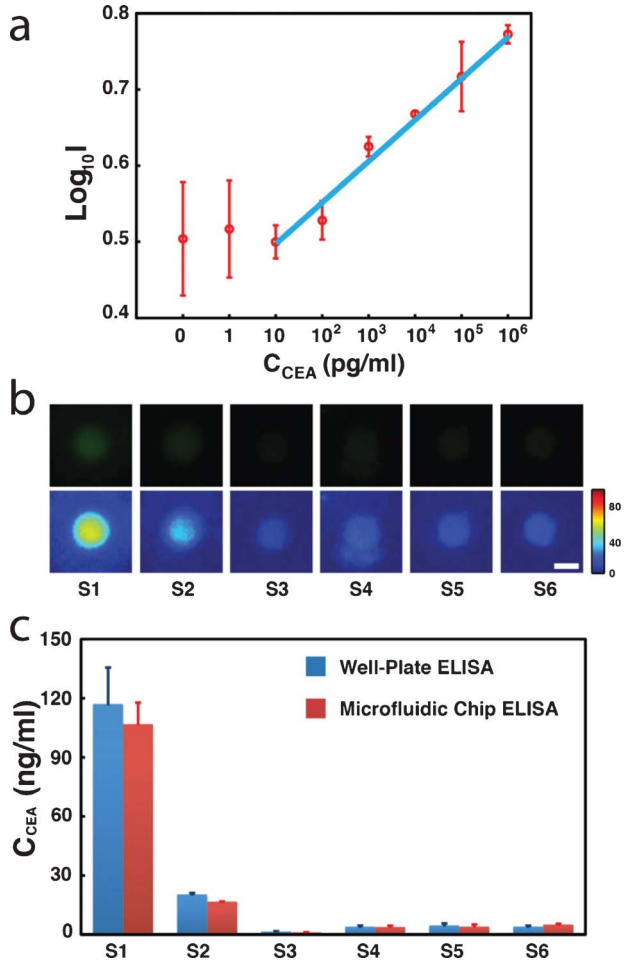

Fig. 4 The sandwich immunoassay of CEA. (a) The sandwich immunoassay of standard CEA samples with different concentration. (b) The fluorescence images (upper row) and processed color maps (lower row) of 6 patient serum samples. Scale bar is 100 μm. (c) The measured CEA concentration using both chip-based and conventional sandwich immunoassays (n = 3).

samples from patients, we have reached comparable results with conventional assays, with improved reproducibility and greatly reduced sample consumption. The dynamic range, the detection limit, the low consumption of sample and reagents, as well as the short time needed for measurement of this chip-based method meet the general requirements of clinical diagnostics. We envision that this method has great potential for high-throughput immunoassays and controllable surface pattering.

Acknowledgements

This research was supported by grants from the National Natural Science Foundation of China (20890020 and 90913011 to Y. H.; 20905004 to Y.P.), the Ministry of Science and Technology of China (200GAA042309 and 2011CB809106 to Y.H.), the Fok Ying Tung Educational Foundation to Y. H., and the Novo Nordisk-CAS Research Foundation (NNCAS-2010-5) to Z. G.

References

1 C. D. Chin, T. Laksanasopin, Y. K. Cheung, D. Steinmiller, V. Linder, H. Parsa, J. Wang, H. Moore, R. Rouse, G. Umviligihozo, E. Karita, L. Mwambarangwe, S. L. Braunstein, J. van de Wijgert, R. Sahabo, J. E. Justman, W. El-Sadr and S. K. Sia, *Nat. Med.*, 2011, **17**, 1015–1019.
2 R. M. Lequin, *Clin. Chem.*, 2005, **51**, 2415–2418.
3 B. S. Ferguson, S. F. Buchsbaum, T. T. Wu, K. Hsieh, Y. Xiao, R. Sun and H. T. Soh, *J. Am. Chem. Soc.*, 2011, **133**, 9129–9135.
4 B. Zheng, L. S. Roach and R. F. Ismagilov, *J. Am. Chem. Soc.*, 2003, **125**, 11170–11171.
5 L. F. Cheow, S. H. Ko, S. J. Kim, K. H. Kang and J. Han, *Anal. Chem.*, 2010, **82**, 3383–3388.
6 W. T. Liu, L. Zhu, Q. W. Qin, Q. Zhang, H. Feng and S. Ang, *Lab Chip*, 2005, **5**, 1327–1330.
7 J. C. McDonald, S. J. Metallo and G. M. Whitesides, *Anal. Chem.*, 2001, **73**, 5645–5650.
8 B. S. Lee, Y. U. Lee, H. S. Kim, T. H. Kim, J. Park, J. G. Lee, J. Kim, H. Kim, W. G. Lee and Y. K. Cho, *Lab Chip*, 2011, **11**, 70–78.
9 G. Acharya, C. L. Chang, D. D. Doorneweerd, E. Vlashi, W. A. Henne, L. C. Hartmann, P. S. Low and C. A. Savran, *J. Am. Chem. Soc.*, 2007, **129**, 15824–15829.
10 T. Thorsen, S. J. Maerkl and S. R. Quake, *Science*, 2002, **298**, 580–584.
11 E. P. Kartalov, J. F. Zhong, A. Scherer, S. R. Quake, C. R. Taylor and W. F. Anderson, *BioTechniques*, 2006, **40**, 85–90.
12 Y. Luo, F. Yu and R. N. Zare, *Lab Chip*, 2008, **8**, 694–700.
13 J. Kong, L. Jiang, X. Su, J. Qin, Y. Du and B. Lin, *Lab Chip*, 2009, **9**, 1541–1547.
14 X. Jiang, J. M. Ng, A. D. Stroock, S. K. Dertinger and G. M. Whitesides, *J. Am. Chem. Soc.*, 2003, **125**, 5294–5295.
15 D. Yang, X. Niu, Y. Liu, Y. Wang, X. Gu, L. Song, R. Zhao, L. Ma, Y. Shao and X. Jiang, *Adv. Mater.*, 2008, **20**, 4770–4775.
16 Y. X. Chen, G. Triola and H. Waldmann, *Acc. Chem. Res.*, 2011, **44**, 762–773.
17 X. Zhou, F. Boey, F. Huo, L. Huang and H. Zhang, *Small*, 2011, **16**, 2273–2289.
18 T. Ekblad and B. Liedberg, *Curr. Opin. Colloid Interface Sci.*, 2010, **15**, 499–509.
19 A. Calabretta, D. Wasserberg, G. A. Posthuma-Trumpie, V. Subramaniam, A. v. Amerongen, R. Corradini, T. Tedeschi, S. Sforza, D. N. Reinhoudt, R. Marchelli, J. Huskens and P. Jonkheijm, *Langmuir*, 2011, **27**, 1536–1542.
20 A. Cerf, B. R. Cipriany, J. J. Benitez and H. G. Craighead, *Anal. Chem.*, 2011, **83**, 8073–8077.
21 J. L. Wilbur, A. Kumar, H. A. Biebuyck, E. Kim and G. M. Whitesides, *Nanotechnology*, 1996, **7**, 452–457.
22 A. Perl, D. N. Reinhoudt and J. Huskens, *Adv. Mater.*, 2009, **21**, 2257–2268.
23 J. C. Love, L. A. Estroff, J. K. Kriebel, R. G. Nuzzo and G. M. Whitesides, *Chem. Rev.*, 2005, **105**, 1103–1169.
24 S. R. Khetani and S. N. Bhatia, *Nat. Biotechnol.*, 2008, **26**, 120–126.
25 L. Li, J. R. Klim, R. Derda, A. H. Courtney and L. L. Kiessling, *Proc. Natl. Acad. Sci. U. S. A.*, 2011, **108**, 11745–11750.
26 D. B. Wheeler, A. E. Carpenter and D. M. Sabatini, *Nat. Genet.*, 2005, **37**, S25–S30.
27 H. Zhang, Y. Hao, J. Yang, Y. Zhou, J. Li, S. Yin, C. Sun, M. Ma, Y. Huang and J. J. Xi, *Nat. Commun.s*, 2011, **2**, 554.
28 A. Chaubey, K. J. Ross, R. M. Leadbetter and K. J. L. Burg, *J. Biomed. Mater. Res., Part B*, 2008, **84B**, 70–78.
29 G. M. Whitesides, E. Ostuni, S. Takayama, X. Jiang and D. E. Ingber, *Annu. Rev. Biomed. Eng.*, 2001, **3**, 335–373.
30 M. A. Unger, H. P. Chou, T. Thorsen, A. Scherer and S. R. Quake, *Science*, 2000, **288**, 113–116.
31 S. J. Maerkl and S. R. Quake, *Science*, 2007, **315**, 233–237.
32 T. J. Collins, *BioTechniques*, 2007, **43**, 25–30.
33 J. C. McDonald, D. C. Duffy, J. R. Anderson, D. T. Chiu, H. Wu, O. J. Schueller and G. M. Whitesides, *Electrophoresis*, 2000, **21**, 27–40.
34 S. Y. Seong, *Clin. Diagn. Lab. Immunol.*, 2002, **9**, 927–930.
35 N. Laboria, A. Fragoso, W. Kemmner, D. Latta, O. Nilsson, M. Luz Botero, K. Drese and C. K. O'Sullivan, *Anal. Chem.*, 2010, **82**, 1712–1719.

Supporting Information

High-throughput Immunoassay through In-channel Microfluidic Patterning

Chunhong Zheng,[a,b] Jingwen Wang,[a] Yuhong Pang,[a,b] Jianbin Wang,[a] Wenbin Li,[c] Zigang Ge,*[,a] and Yanyi Huang*[,a,b]

[a] *College of Engineering, Peking University, Beijing 100871, China*

[b] *Biodynamic Optical Imaging Center (BIOPIC), Peking University, Beijing 100871, China*

[c] *Beijing Shijitan Hospital, and College of Oncology, Capital Medical University, Beijing 100038, China*

**Corresponding authors: Y. H. (yanyi@pku.edu.cn), and Z. G. (gez@pku.edu.cn)*

Experimental Section

Fabrication of micro-immunoassay chip. We fabricated micro-immunoassay chips using multi-layer soft lithography technology. In brief, we fabricated the molds for the fluidic channels and control channels through photolithography. The mold of the control channels was made from 20 μm-thick negative photoresist (SU8-2010, MicroChem, Newton, MA, USA) patterned on a silicon wafer. The mold of fluidic channels was made from positive photoresist (P4620, AZ Electronic Materials, Branchburg, NJ, USA). The fluidic channel was rounded after reflow and its height was about 14 μm. We used PDMS (Sylgard 184, Dow Corning, Michigan, USA) to fabricate the chips. All molds were exposed to chlorotrimethylsilane (TMCS) vapor for 10 min before PDMS casting. The control layer was made from the PDMS with component ratio of 5:1, while the fluidic layer was made of the PDMS with component ratio 23:1. These two layers were bonded together by baking at 80 °C for 30 min in an oven. The assembled two-layer structure was finally placed on an epoxide glass slide (CEL, Arrayit, USA) and then baked in an oven at 80 °C overnight to strengthen bonding.

Materials. Human IgG, Goat anti Human IgG labeled with FITC, polyclonal rabbit anti Human IgG, monoclonal mouse anti Human IgG and polyclonal rabbit anti Human CEA were purchased from Bioscience. Tris-base, BSA and PEG2000 were obtained from Sigma. Monoclonal mouse anti Human CEA and Human CEA standard sample were purchased from Fizrald.

Condition optimization. When we identified blocking buffers' effect to the background signal, we treated each channels with different blocking buffer in parallel using a single chip. After incubating for 10 min, we washed those channels thoroughly with PBS, and then filled the channels with FITC-labeled goat anti-human IgG and incubated for 15 min. After another PBS washing step, we captured the fluorescence images of the channels for analysis. In this process we did not press the buttons for any assays.

Sample preparation and immunoassays. We tested the patient sera in 2X serial dilution using PBS and found that when the sample is diluted once (1:1) the signal-to-noise ratio was the best. We introduced PBS with 1% BSA and 10 mM Tris buffered saline into the microchannels as the blocking buffer, and incubated for 10 min at 25 ^{o}C to block the non-reactive area. We then washed all the channels with PBS for 3 min while kept the button activated. We then released the button valves to expose the unprotected patterns,

and filled the channels with 500 μg ml^{-1} capture antibody, incubated for 15 min at 25 ^{o}C. After the reaction, we washed the channel again with PBS buffer for 3 min. The samples were then loaded into the microchannels and incubated for 15 min at 25 ^{o}C. We later washed the channels with PBS for 3 min. Finally, we filled the channels with 125 μg ml^{-1} detecting antibody and incubated for 10 min at 25 ^{o}C. After PBS washing for 3 min, we took fluorescence images for quantitative analysis.

Image acquisition. An Olympus BX51 upright fluorescence microscope was used for observing and a TuSen CCD (TCC-1.4HICE) was used to capture images. All data was analyzed using Image J and MATLAB.

Table S1. The relationship between the concentration of capture antibody and the detection limit of antigen using sandwich ELISA

Capture antibody concentration (μg ml^{-1})	Antigen detection limit (ng ml^{-1})
0~31.25	>20
62.5	2~20
125	≥0.02
250~1000	≤0.02

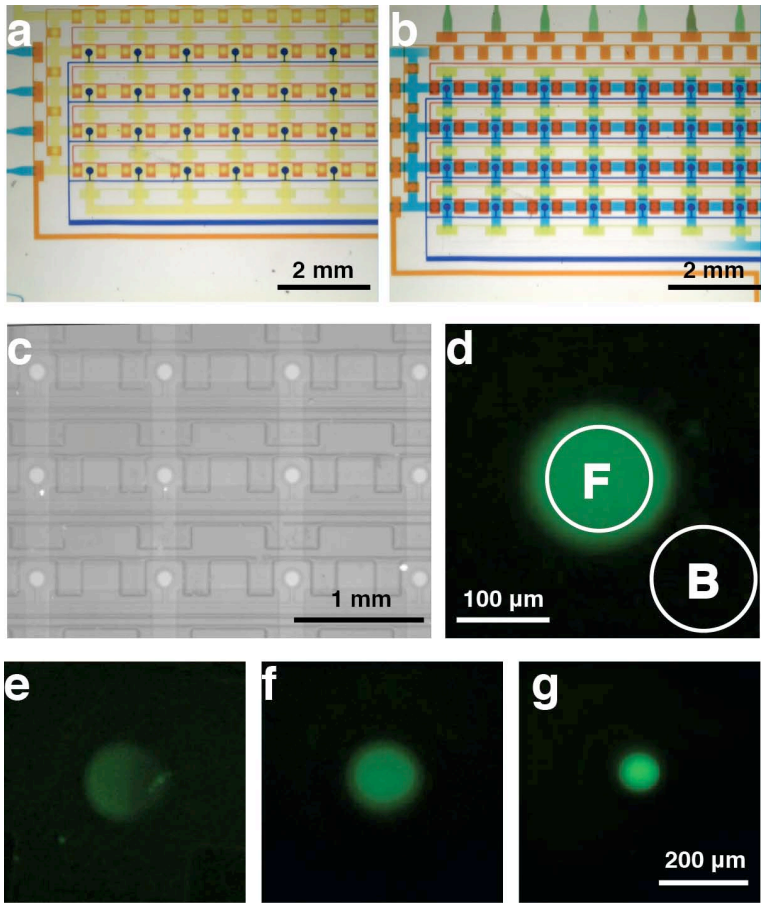

Figure S1. (a) The illustration of blocking process. The blue button valve (blue circle) is activated to protect reaction area. Blocking buffer (yellow solution) cannot access these spots. (b) The illustration of antigen-antibody binding step. The button valve is inactivated and reaction is carried out on the capture-antibody-patterned spots. (c) The array of fluorescent spots from fluorescence ELISA reactions. (d) The image processing of each reaction chamber. The central part of the fluorescent area is cropped with a round-shape mask as the signal, and the non-reaction area is also cropped with the mask of same size for background subtraction. The intensity of each spot was determined by integrating all pixels inside the circle, to minimize the error generated from image noise. (e) The pear-shape fluorescence pattern when button is over-pressurized. (f) The properly pressurized button valve generates a perfect circular reaction area. (g) When the button valve is under-pressurized, the spot size will be reduced. Scale bar is 200 µm.

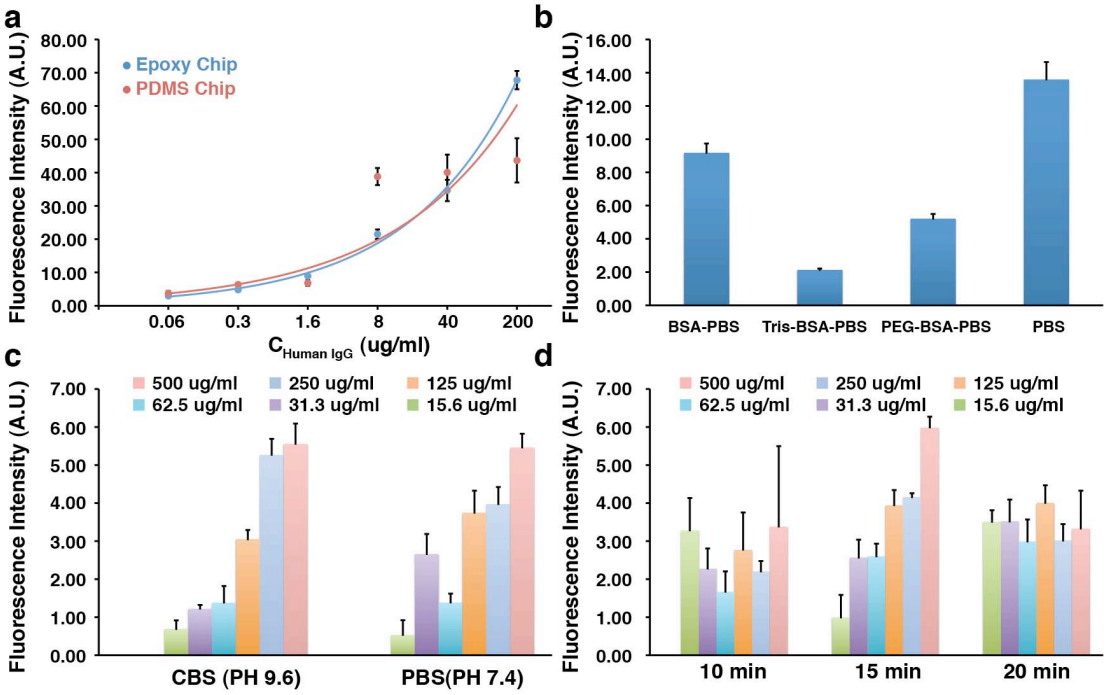

Figure S2. (a) The signal intensity – antigen concentration working curves obtained from the identical designed chips with different substrate. The fitting curve (blue line) for epoxide glass substrate has a high R-square value, 0.99, while the fitting curve (red line) for PDMS substrate has a low R-square value, 0.87. (b) The effect of different blocking buffer. The blocking buffer containing 1% BSA and 10 mM Tris buffered saline shows the best performance. (c) The effect of reaction/dilution buffer. Antigen diluted with carbonate buffer solution (CBS) appears in a normal rising with concentration increasing. This is probably because CBS is slightly basic and hence facilitate the coupling reactions in the immunoassays. (d) The effect of incubation time for immunoglobulin adsorption. The antigen-antibody conjugation is dynamic. Through the experiments we found that 15-min incubation was a proper choice, and the data showed the correct tendency with different concentrations. If the incubation time is too short or too long, the under- or over-adsorption may introduce the artifacts, leading to false determination of the concentrations and large errors between the replicates.

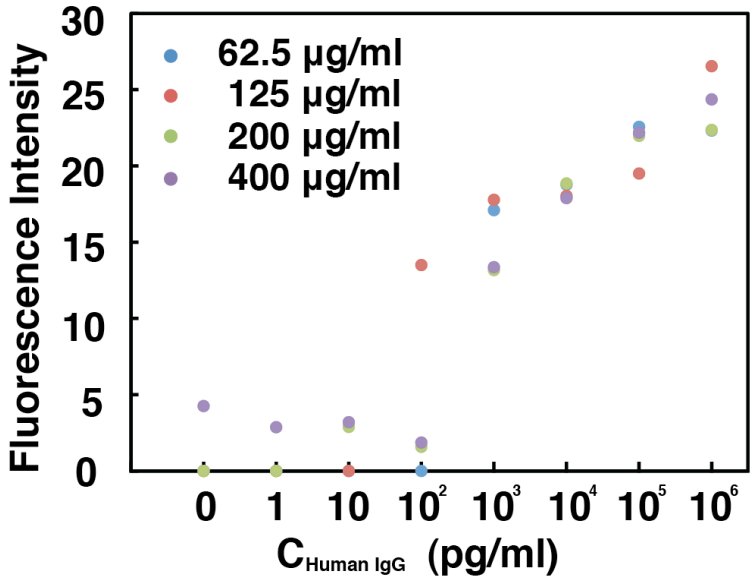

Figure S3. The checkerboard titration for determining the proper concentration of detecting antibody. The capture antibody is 500 µg ml^{-1} mouse anti human IgG monoclonal antibody. The human IgG was diluted from 1 µg ml^{-1} to 1 pg ml^{-1}. The concentrations of detecting antibody are 62.5 µg ml^{-1} (blue), 125 µg ml^{-1} (red), 200 µg ml^{-1} (green), and 400 µg ml^{-1} (purple). During titration we found that when the concentration of Human IgG was too low (10 pg/ml or lower), the intensity difference between the button areas and the background was hard to identify. The data points at this low-concentration range are majorly artifacts, as shown in Fig. S3. In this experiment, 125 µg ml^{-1} detecting antibody has a detection limitation at about 100 pg/ml. With different experimental conditions and different antibodies, this limit may vary.

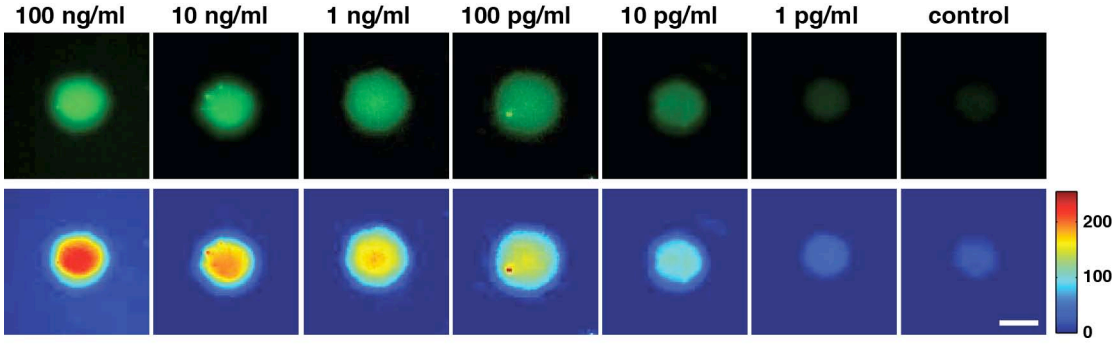

Figure S4. The images of the sandwich ELISA reaction spots with different concentration of human IgG. Capture antibody is 500 μg ml^{-1} mouse anti human IgG monoclonal antibody, and detecting antibody is 125 μg ml^{-1} rabbit anti human IgG polyclonal antibody. The upper row is the original fluorescent pictures and the lower row is the corresponding color maps. Scale bar is 200 μm.

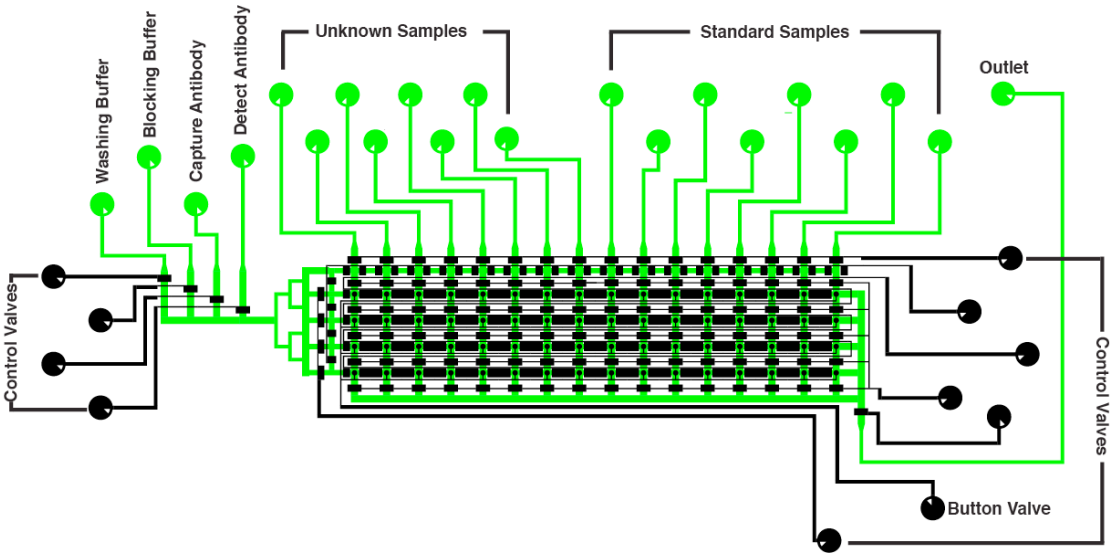

Figure S5. An improved version of microfluidic immunoassay chip. This chip is designed for human CEA detection. The green layer is the fluidic layer, and the black layer is the control layer. The left four inlets are designed for introducing the common reagents, including washing buffer, blocking buffer, capture antibody and detecting antibody. Sixteen inlets on the top part are designed for introducing unknown samples and CEA standard samples.